Title
Molecular mechanism of water reorientational slowing down in concentrated ionic solutions.

Journal
Proceedings of the National Academy of Sciences of USA, 114(38)

Authors
Zhang, Qiang
Wu, TianMin
Chen, Chen
et al.

Publication Date
2017-09-19

DOI
10.1073/pnas.1707453114

Peer reviewed

Molecular mechanism of water reorientational slowing down in concentrated ionic solutions

Qiang Zhang[a,b,c], TianMin Wu[a], Chen Chen[b], Shaul Mukamel[d,1], and Wei Zhuang[a,1]

[a]State Key Laboratory of Structural Chemistry, Fujian Institute of Research on the Structure of Matter, Chinese Academy of Sciences, Fuzhou, Fujian 350002, China; [b]Department of Chemistry, Bohai University, Jinzhou 121013, China; [c]Fujian Provincial Key Laboratory of Theoretical and Computational Chemistry, Xiamen, Fujian 361005, China; and [d]Department of Chemistry, University of California, Irvine, CA 92697

Contributed by Shaul Mukamel, August 10, 2017 (sent for review May 8, 2017; reviewed by Huib J. Bakker and Dongping Zhong)

Water dynamics in concentrated ionic solutions plays an important role in a number of material and energy conversion processes such as the charge transfer at the electrolyte–electrode interface in aqueous rechargeable ion batteries. One long-standing puzzle is that all electrolytes, regardless of their "structure-making/breaking" nature, make water rotate slower at high concentrations. To understand this effect, we present a theoretical simulation study of the reorientational motion of water molecules in different ionic solutions. Using an extended Ivanov model, water rotation is decomposed into contributions from large-amplitude angular jumps and a slower frame motion which was studied in a coarse-grained manner. Bearing a certain resemblance to water rotation near large biological molecules, the general deceleration is found to be largely due to the coupling of the slow, collective component of water rotation with the motion of large hydrated ion clusters ubiquitously existing in the concentrated ionic solutions. This finding is at variance with the intuitive expectation that the slowing down is caused by the change in fast, single-molecular water hydrogen bond switching adjacent to the ions.

ion specificity | water rotation | ionic solution | femtosecond infrared | structure dynamics

The dynamics of water molecules surrounding hydrated ions and ionic moieties plays an important role in a broad range of chemical and biological phenomena (1–6). In protein solutions, for example, amino acids with charged side chains strongly affect the water motion in their vicinity, which consequently impacts various protein biological processes such as enzyme catalysis and folding (3–5). As another example, chemical reactions with ionic reactants can be driven by the kinetic energy transferred from the surrounding water molecules (7). Many material design and energy conversion processes are related to the ion effect in the concentrated aqueous solutions (8). High concentration (>1 M) solutions with the cations such as Li^+, Na^+, Mg^{2+}, Ca^{2+}, Zn^{2+}, and Al^{3+} are used as electrolytes in aqueous rechargeable ion batteries, a promising green alternative of the conventional organic electrolyte-based batteries (9, 10). Important questions such as how the charge transfer at the electrolyte–electrode interface correlates with the nearby solvent dynamics and how this correlation is impacted by the hydrated ions are yet to be quantitatively understood (9, 10).

Ion effects in concentrated solutions are much less understood (1, 11–14) than ideal dilute solutions. The concept of structure makers (ions that enhance the water hydrogen-bonding structure) and breakers (ions that weaken the water hydrogen-bonding structure) has been generally applied to rationalize the ion-specific impacts on water dynamics in dilute ionic solutions (15). In concentrated solutions, in contrast, all electrolytes slow down the water rotation regardless of their structure-making/breaking natures (11–14). Resolving this intriguing issue is crucial for developing a consistent molecular picture of the ion impact on water dynamics.

One could reason that it is the altered water hydrogen-bond–switching behavior around the ions that leads to this general retardation (11) (Fig. 1*B*): Water rotation has contributions from large-amplitude angular jumps during the exchange of hydrogen bond acceptors as well as slower frame reorientations of the intact hydrogen bond axis (15). The latter is dominant in concentrated solutions. Neutron scattering measurements reveal that the ions enhance the probability to find water molecules which act as the hydrogen bond acceptors in an interstitial position between the first and second hydration shells in pure water (16). Some water molecules adjacent to the ions therefore stride over a markedly shorter distance during the hydrogen bond switching, which decelerates the water diffusion and consequently the overall water rotation. This intuitive picture implies a local involvement of ion effects on the water molecules only in its immediate vicinity.

We report a theoretical study of the molecular mechanism of this retardation, which employs a continuous-time random-walk (CTRW) coarse-graining method (17) and combines numerical simulations with the extended Ivanov jump model (11, 15). The rotational time of water is obtained by fitting the second-order reorientation correlation function (Eq. **S1** in *Supporting Information*) with single-exponential function (11, 15, 18). We find that, surprisingly, the general deceleration is significantly impacted by the influence of the ions on the nonlocal water structure dynamics, which is the rearrangement dynamics of water hydrogen bond networks involving the slow collective motions of many water molecules, accompanied by large energy fluctuations (19). Further analysis indicates that, at higher concentrations, all ions, regardless of their structure-making/breaking propensity, deviate from the ideal solution picture by associating into clusters. Collective water rotation is then retarded due to its coupling with the slow dynamics of ion clusters (Fig. 1*C*).

Significance

The dynamics of water molecules surrounding the hydrated ions affects many natural phenomena including protein processes and charge transfer in the aqueous rechargeable ion batteries. In the concentrated solutions, a long-standing puzzle is that all electrolytes retard water rotation regardless of whether they weaken or strengthen the water hydrogen-bonding network. We investigate this issue theoretically and find the deceleration to be largely due to the coupling of the slow, collective component of water rotation with the motion of sizable ion clusters in the concentrated solutions. This finding is at variance with the intuitive expectation that the deceleration is caused by the change in fast, single-molecular water hydrogen bond switching adjacent to the ions.

Author contributions: W.Z. designed research; Q.Z., C.C., and W.Z. performed research; T.W., S.M., and W.Z. analyzed data; and W.Z. wrote the paper.

Reviewers: H.J.B., Fundamental Research on Matter Institute for Atomic and Molecular Physics; and D.Z., Ohio State University.

The authors declare no conflict of interest.

[1]To whom correspondence may be addressed. Email: wzhuang@fjirsm.ac.cn or smukamel@uci.edu.

This article contains supporting information online at www.pnas.org/lookup/suppl/doi:10.1073/pnas.1707453114/-/DCSupplemental.

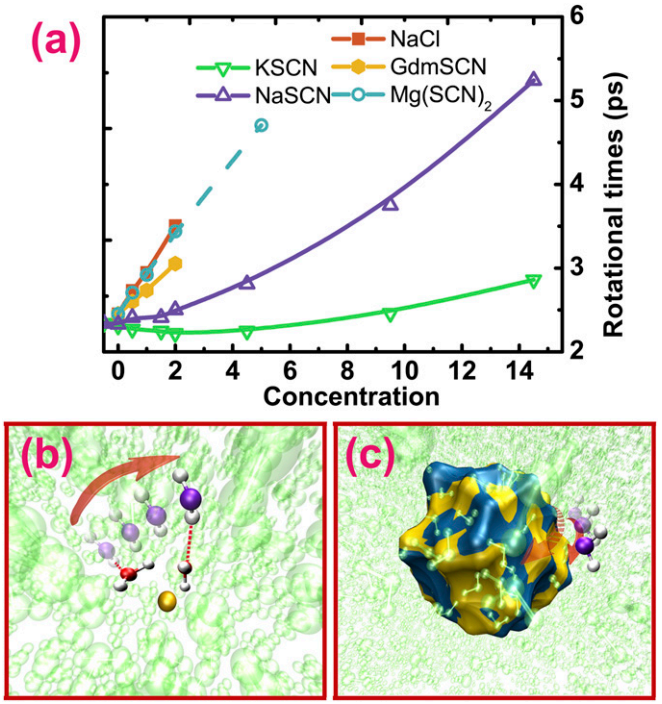

Fig. 1. (*A*) Rotational times of water in NaCl (the saturated concentration: ~6 M), GdmSCN (guanidinium thiocyanate, the saturated concentration: unknown), $Mg(SCN)_2$ (the saturated concentration: unknown), KSCN (the saturated concentration: ~18 M), and NaSCN (the saturated concentration: ~17 M) aqueous solutions at different concentrations. (*B* and *C*) Schematic representations of two possible molecular mechanisms leading to the deceleration of water rotation in the concentrated ionic solutions: in *B*, an ion (gold) enhances the probability for a target water molecule (purple) to find the next hydrogen bond acceptor water molecule, which decelerates the water diffusion and consequently the overall water rotation. In *C*, ions associate into the cluster. Water frame rotation is retarded due to its coupling with the slow dynamics of the ion clusters.

Ion clustering in solutions at finite concentrations has been a topic under debate due to the diverse time and spatial resolutions of detecting techniques as well as computer simulations (1, 12, 14, 20, 21). Recently, femtosecond infrared vibrational energy exchange and anisotropy measurements (12) have emerged as a powerful tool for probing the ion association and clustering at the timescale directly comparable with the computer simulation (18, 22, 23). Our simulations on KSCN and GdmSCN, using the same theoretical setup as in the current work, produced solution structure features qualitatively consistent with the experiments, which includes the clustering percentage of KSCN at different concentrations (table 1 in ref. 12) and the radial distribution functions in GdmSCN solutions (22).

Results and Discussion

General Concentration-Dependent Slowing Down. The cations/anions of the electrolytes NaCl, GdmSCN, NaSCN, KSCN, and MgSCN have different structure-making/breaking natures (24). Our simulations (details are given in section 1 of *Supporting Information* and Table S1; the rotational times of water are calculated as in section 2 of *Supporting Information*) show that water rotation in all these systems slows down in concentrated solutions (Fig. 1*A*). This is consistent with many other reports (11, 21, 23, 24). In the following, we explore the underlying mechanism of this retardation.

We focus on NaSCN and KSCN. The simulated second-order rotational correlation functions of water in KSCN and NaSCN solutions from 2.5 to 15 M are shown in Fig. 2. The simulation results, consistent with the previous experiments, deviates from single-exponential behavior (23). To evaluate the ion effects, a procedure based on the extended Ivanov jump model (11, 15) (details in section 3 of *Supporting Information*) was used. The trajectory of each water molecule is dissected into a series of hydrogen-bond–switching steps. These events are then regrouped into four categories according to the initial and final hydrogen bond acceptors: (*i*) water to water (*W*:*W*); (*ii*) water to *SCN* (*W*:*SCN*); (*iii*) *SCN* to water (*SCN*:*W*); and (*iv*) *SCN* to *SCN* (*SCN*:*SCN*). The overall difference between the rotation time constant of water in solution with a finite concentration and that in very dilute solution (0.1 M) is decomposed into the jump and frame contributions of all four switching types according to Eq. **1**:

$$\tau(c)-\tau(0)=\delta\tau_P+\delta\tau^J_{W:W}+\delta\tau^f_{W:W}+\delta\tau^J_{W:SCN}+\delta\tau^f_{W:SCN}+\delta\tau^J_{SCN:W}+\delta\tau^f_{SCN:W}+\delta\tau^J_{SCN:SCN}+\delta\tau^f_{SCN:SCN}. \quad [1]$$

The first term $\delta\tau_p$ represents the contribution from replacing the *W*:*W* type of hydrogen bond switching in pure water with the anion-related types (*SCN*:*W*, *W*:*SCN*, and *SCN*:*SCN*) in solution, assuming that each type makes a concentration-independent contribution to the overall rotation. Each of the remaining eight terms in Eq. **1** describes how the jump or frame rotation of the water molecule, during a hydrogen bond switching, is affected by ions (section 4 of *Supporting Information*). All of the nine contributions are given in Fig. S1. The strongest ion influences are on the jump and frame contributions of *W*:*W* type [$\delta\tau^J_{W:W}$ and $\delta\tau^f_{W:W}$ have the most significant contributions to $\tau(c)-\tau(0)$]. Fig. 2 presents $\delta\tau^J_{W:W}$ and $\delta\tau^f_{W:W}$ at a series of concentrations. Adding ions accelerates the jump rotation ($\delta\tau^J_{W:W}<0$), while the retarding trend of the overall water rotation mainly originates from the frame component ($\delta\tau^f_{W:W}>0$). This is consistent with previous observations on other electrolytes (11). We next examine why the frame component significantly slows down in concentrated solutions.

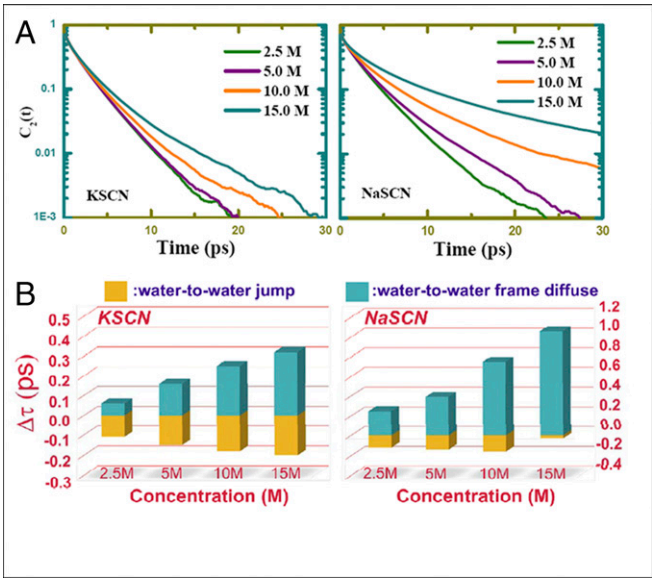

Fig. 2. (*A*) The simulated second-order rotational correlation functions of water in KSCN (*Left*) and NaSCN (*Right*) solutions. (*B*) Concentration-dependent ion effects on the jump and frame rotation time constants during the *W*:*W* hydrogen-bond–switching processes ($\delta\tau^J_{W:W}$ and $\delta\tau^f_{W:W}$ in Eq. **1**) for the concentrated *KSCN* (*Left*), and *NaSCN* (*Right*) solutions.

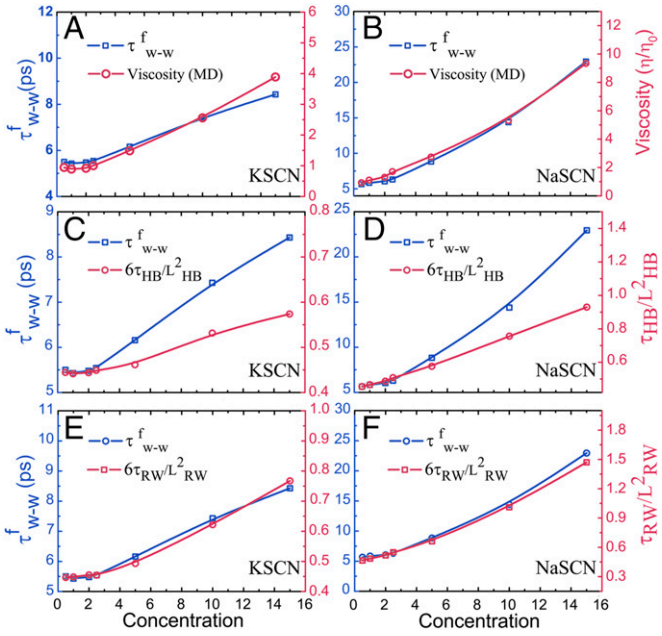

Fig. 3. Correlation plots between τ^f_{W-W} and the calculated relative viscosity η/η_0 (*A* and *B*), $6\tau_{HB}/L^2_{HB}$ (*C* and *D*), and $6\tau_{RW}/L^2_{RW}$ (*E* and *F*) with the unit of $(10^{-5}$ cm/s$)^{-1}$.

The Influence of Altered Hydrogen-Bond–Switching Behavior. Consistent with Stokes–Einstein relation (25), a correlation is observed between the calculated frame rotation time τ^f_{W-W} and viscosity (Fig. 3 *A* and *B*). According to the Eyring model (25), τ^f_{W-W} is then proportional to τ_{HOP}/L^2_{HOP}, where τ_{HOP} and L_{HOP} are the time and length scales of the "excited hoppings" of molecules or collections of molecules from one "local basin" to another (17). As the solution becomes more concentrated, these time and length scales change, which lead to slower water rotational diffusion (e.g., higher τ^f_{W-W}). Clarifying the nature of these hoppings should help unravel the molecular mechanism of the frame retardation.

We first assume that τ_{HOP} represents the water hydrogen-bond–switching time τ_{HB} (Fig. 4*A*) and L_{HOP} is the switching length L_{HB} during τ_{HB}. The distributions of L_{HB} and τ_{HB} in pure water and in 5 M solutions are shown in Fig. 4 *C* and *E*. The values of τ_{HB}/L^2_{HB} only correlate with τ^f_{W-W} up to a fairly low concentration (Fig. 3 *C* and *D*). At higher concentrations, this picture seriously underestimates the retardation of the frame rotation.

Neutron-scattering and computer simulation studies have suggested that water "structural dynamics," the collective rearrangements of the H-bond network, has two motional components: picosecond local structural fluctuations within dynamical basins and slower interbasin hoppings (11, 17, 25). To examine the correlation of these hoppings with the frame deceleration, we used a CTRW model (17) to qualitatively evaluate their spatial and temporal characteristics (section 1 of *Methods* section and section 5 of *Supporting Information*). A schematic representation is presented in Fig. 4*B*. Briefly, for a single water molecule, its running average position $\mathbf{R}(n)$ of n consecutive frames along the molecular dynamics (MD) trajectory is computed by averaging its center of mass. If the separation between $\mathbf{R}(n)$ and $\mathbf{R}(n+1)$ is beyond the prescribed distance D_{max}, it is assumed that a jump translation has occurred between frame n to $n+1$. The water molecule had jumped into another dynamic basin at the $n+1$ frame. The n consecutive frames are identified as a "dynamical basin" centered at $\mathbf{R}(n)$. The counter $n+1$ is reset to 1 for the next dynamic basin. Fig. 4*B* shows the position of the molecular center of mass of a chosen water molecule during 100 ps in a 5 M solution. The trajectory exhibits a pronounced clustering with well-defined dynamical basins (represented schematically in different colors).

We can define τ_{HOP} as the average waiting time τ_{RW} of water within the dynamic basins, while L_{HOP} is the distance L_{RW} between any two consecutive basin center, and $D_{max} = 1.5$ Å was used in previous work for water (25). A strong correlation between τ_{RW}/L^2_{RW} and τ^f_{W-W} is observed (Fig. 3 *E* and *F*). It is therefore the ion effect on the collective water motion that drives the general slowdown observed. The distributions of L_{RW} and τ_{RW} for the pure water and NaSCN solutions at 5 M are shown in Fig. 4 *D* and *F*, which are much larger than τ_{HB} and L_{HB}. Distribution of τ_{HB} is much more inhomogeneous. Maximum of τ_{HB} distribution appears around 0.5 ps. The average value reaches 2.271 because of the very long tail. On the other hand, τ_{RW} has a much broader but more homogeneous distribution which centers around $\tau_{RW} = 2.0$ ps.

Van Hove Distribution of Water Rotational Dynamics. To demonstrate more directly the deceleration mechanism, we have further calculated the rotational van Hove distribution function (26):

$$G_R(\varphi,t) = \left\langle \frac{1}{N}\sum_{i=1}^{N} \delta\left(\left|\vec{\varphi}_i(t) - \vec{\varphi}_i(0)\right| - \varphi\right)\right\rangle. \quad [2]$$

Here, $\langle\cdots\rangle$ represents the average over configurations. This function gives the average probability to find a particle rotate over an angle of $\vec{\varphi}_i$ within the time interval t. For a

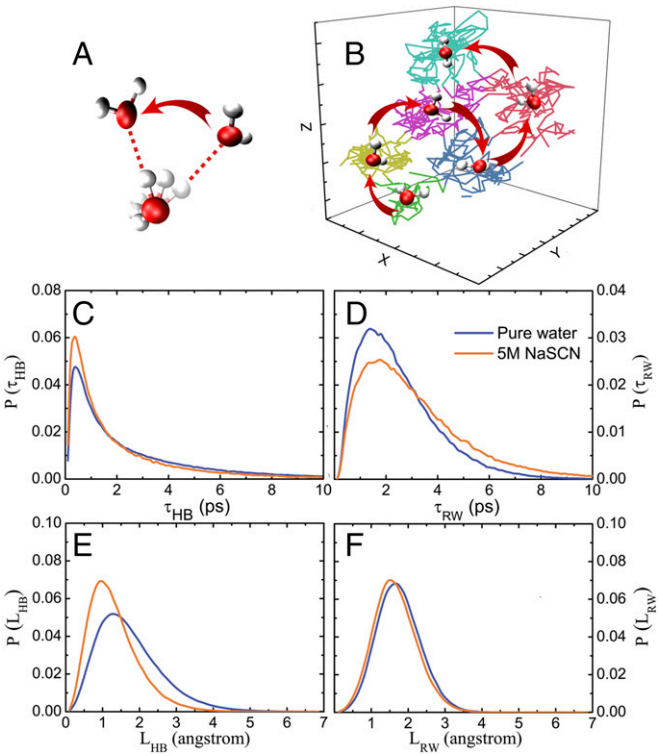

Fig. 4. Two possible "hopping" mechanisms. The schematic picture of the hydrogen bond switching (*A*) and the collective water dynamics (*B*). The distributions of hopping time (*Middle* row) and length (*Bottom* row) of water molecule are presented for pure water (blue) and 5 M NaSCN solutions (orange) in the hydrogen bond switching (*C* and *E*) and collective dynamics (*D* and *F*) picture, respectively.

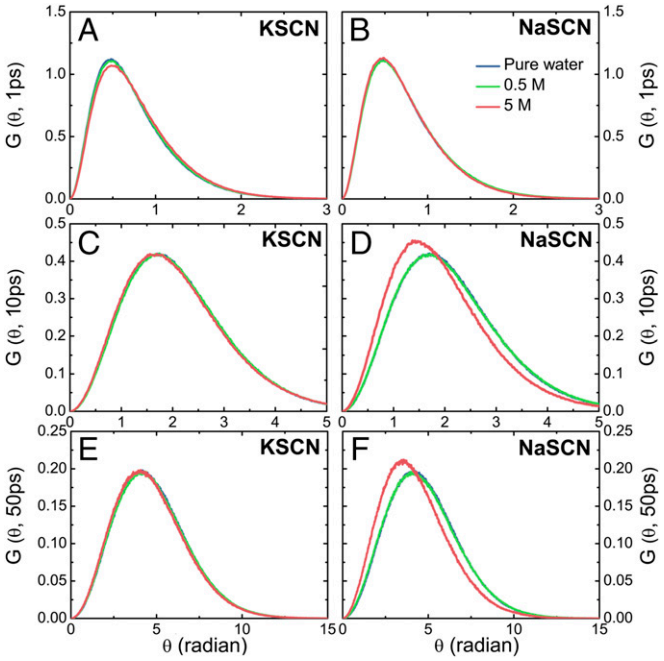

Fig. 5. Van Hove distribution functions of water rotation at the time intervals of 1 (*A* and *B*), 10 (*C* and *D*), and 50 (*E* and *F*) ps in pure water, the KSCN and NaSCN solution at 0.5 and 5 M.

homogeneous rotational dynamics, $G_R(\phi,t)$ converges to a Gaussian form:

$$G_0(\phi,t)=\left[\frac{3}{2\pi\langle\phi^2(t)\rangle}\right]^{3/2}\exp\left[-3\phi^2/2\langle\phi^2(t)\rangle\right]. \quad [3]$$

The deviation of $G_R(\phi,t)$ from the Gaussian form $G_0(\phi,t)$ can be quantified by the parameter:

$$\alpha_2(t)=3\langle\phi^4(t)\rangle/5\langle\phi^2(t)\rangle^2-1, \quad [4]$$

which represents the dynamic heterogeneity at a certain moment t (Fig. S2). The rotational van Hove distribution functions at t = 1, 10, and 50 ps are presented in Fig. 5 for pure water and 0.5 and 5 M solutions. Fig. 5 gives the time dependence of $\alpha_2(t)$ within 100 ps. The method is explained in detail in section 2 of *Methods* and section 6 of *Supporting Information*.

At t = 1 ps, the presence of the ions does not lead to significant differences in the rotational distributions. Ion effects on fast processes such as water libration, jump rotation, and subpicosecond diffusion, therefore, do not contribute significantly to the retardation in concentrated solutions. Large heterogeneity appears within 1 ps, which is consistent with previous observations that the fast dynamics of water in different local hydrogen-bonding environments is fairly inhomogeneous (13, 18, 19, 27).

At t = 10 ps, the distribution functions of NaSCN show a clear concentration dependence, water rotation in the 5 M solution is much slower than that in pure water and the 0.5 M solution. This timescale indicates that the deceleration of water rotation in the concentrated ionic solution is due to the change of its collective diffusion components which is at the picosecond timescale (11, 15, 19). Fig. 4 suggests a typical residence time t_{res} of ~3 ps for water in the dynamical basins during the diffusion. At 10 ps, the collective motion of water molecules has enough time to hop out of a certain basin but not to cover a large number of basins to average out the influence of the initial condition. Van Hove distribution functions therefore have a significantly non-Gaussian shape, which suggests heterogeneity.

At t = 50 ps or longer, water rotation becomes even slower in 5 M solution compared with pure water. Furthermore, since $t \gg t_{res}$, most of the water molecules sample a series of different local environments. The average rotating speeds becomes similar and the van Hove distribution becomes homogeneous with a Gaussian shape.

Water Frame Rotation Is Coupled to the Slow Ion Cluster Dynamics. It is difficult to understand the aforementioned retardation in the ideal solution picture. In fact, in less concentrated (i.e., closer to ideal) solutions, water frame rotation can become faster for some electrolytes and slows down for others (6). On the other hand, collective water motion around the large biomolecules is always retarded comparing to that in pure water (3, 4). These observations imply a correlation between the solute size and the observed retardation.

A number of previous studies had revealed that, at concentrated solutions, the attractive forces between cations and anions overcome the thermal agitation and the ion pairs or clusters start to form (12, 14, 20, 21). We calculated the distribution of the ion cluster sizes for NaSCN and KSCN at 5 M and GdmSCN, $Mg(SCN)_2$, and NaCl at 2 M (saturated) in Table 1 (definition of ion cluster in the section 3 of *Methods* and in the section 7 of *Supporting Information*). Significant clustering is observed in all cases.

Even though polarizable force fields as well as ab initio models might generate results agreeing more quantitatively with experiment (28, 29), they become computationally too expensive for the large systems and long time simulations herein. Additionally, advanced polarizable force field models are often unavailable for many commonly studied ions. Since the ion–water interaction models used herein nicely reproduce the clustering characters measured by the coherent 2D infrared techniques for various electrolytes at a series of concentrations (6, 18, 22, 23), it provides a cost-effective means to describe the clustering phenomenon to the extent needed for our discussion.

Hydration of biomolecules are found to participate in and sometimes directly control their motions (3, 4). On the other hand, biomolecules also influence the collective motions of surrounding water molecules (30). To examine whether a similar coupling happens in the solutions of sizable ion clusters (with 30~50 ions or even larger), we plot in Fig. 6*A* the average rotational time constants for water molecules adjacent to the clusters with different sizes in both *KSCN* and *NaSCN* solutions at 5 M. Water molecules indeed rotate more slowly around larger clusters.

We further estimate the rotation of the ion clusters with different sizes by calculating the populations of their rotation angles using a superposing method (31) (Fig. 6 *B* and *C*). Details are given in section 4 of *Methods* and in section 8 of *Supporting Information*. The average rotational angles of small clusters (with size $2 < N < 10$) and larger clusters (with $N \geq 10$) are calculated separately and compared. Rotations of the larger ion clusters are clearly slower than those of the smaller ones. Collective rotation

Table 1. The populations of ion cluster with the different size in NaCl, GdmSCN, KSCN, NaSCN, and $Mg(SCN)_2$ aqueous solutions

	Population of ion cluster with size N (%)		
Salt	$N = 1$	$1 < N < 10$	$10 \leq N$
NaCl (2 M)	78.85	21.15	0.00
GdmSCN (2 M)	70.47	29.53	0.00
KSCN (5 M)	60.08	31.33	8.59
NaSCN (5 M)	46.97	46.54	6.50
$Mg(SCN)_2$ (2 M)	64.02	35.98	0.00

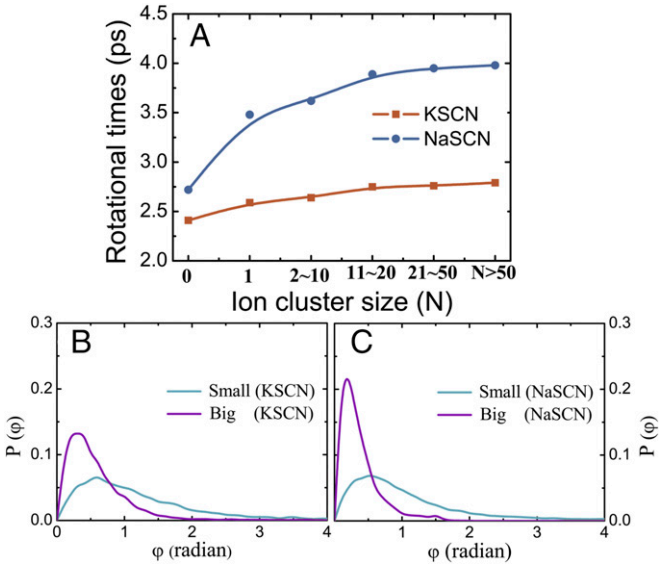

Fig. 6. (*A*) The rotational times of water adjacent to the ion clusters with different sizes, *N*, for $N = 0$, 1, 2–10, 11–20, 21–50, 51– in KSCN and NaSCN solutions at 5 M. (*B* and *C*) The populations of the rotation speed of ion cluster in KSCN and NaSCN solutions at 5 M: the small ion cluster with the size $2 < N < 10$ and the big ion cluster with the size *N* not less than 10.

of water molecules adjacent to larger ion clusters is therefore slower due to the coupling with a more retarded cluster rotation.

To reaffirm that this retardation of overall water rotation around the clusters is mostly attributed to the frame motion, we monitor the motions of the rotationally fastest and slowest 10% of water molecules in the rotational van Hove distribution $G_R(\phi, t)$ in 5 M solutions and in pure water (Fig. 7). Comparing to that in pure water, jump components of the fastest and slowest water in the 5 M solutions are only slightly sped up. Frame components in the solutions, on the other hand, are significantly slower than that in pure water. Furthermore, within the 5 M solutions, the difference between the jump components of fastest and slowest water is minor, while that between the frame components is much more significant. Ion clusters retard water rotation, therefore, mainly by affecting the frame component.

Although larger ion clusters are found in the KSCN solution than in the NaSCN solution at same concentration (Table 1), collective water frame rotation is retarded more significantly in the latter (Fig. 7). This is due to the stronger water affinity of the sodium cations (the average residence time of a water molecule in the cation first solvation shell of is 21.61 ps for sodium, while 65.91 ps for potassium). Since the dependence of the retarding effect on the cluster size becomes less significant for the large clusters (Fig. 6*A*), longer residence time becomes the more important factor of retardation because water couples with the motion of the cluster for longer time.

Conclusions

We had demonstrated that the general retardation of water rotation in concentrated ionic solutions may be largely attributed to ions effect on water structure dynamics. Further analysis reveals that cations and anions in the concentrated solutions start to form clusters. Slow cluster motions couple with water frame rotations nearby and retard the water dynamics. This observation is similar to the retardation of water rotation near large biological molecules measured by fluorescence and terahertz experiments.

Ion-pairing and clustering tendency in the solution correlates with the relative ion–ion, ion–water affinities. Cations which are structure makers tend to pair with maker anions, and so do the breakers. However, at higher concentrations, due to the higher ion/water ratio, clusters exist even when the water affinities of cation and anion are rather mismatched. For instance, a significant portion of the ions form clusters in the aqueous LiSCN solutions (12, 23) with medium to high concentrations. Here, lithium cation is a strong maker while thiocyanate anion is a strong breaker. As another example, ion clusters are found to exist in aqueous Gdm_2SO4 solutions (22). Here, Gdm^+ is a strong breaker while SO_4^{2-} is a strong maker. Big ion aggregates are also found in concentrated NaCl (21) and $CaCO_3$ solutions (32). We therefore believe that our finding is general for other salt solutions.

There have been spectroscopic reports suggesting that ions can affect the collective water rotational dynamics (1, 13, 19, 33). For instance, long time decay in the time domain optical Kerr effect signal of liquid water and aqueous solutions has been assigned to the slow collective water structure dynamics (α relaxation) (33) and is composed of the contributions from both the rotational and translational motions. Through a projection scheme, the rotational component can be separated out and studied in detail. The characteristic relaxation time of the rotational component has been found to be significantly altered with more ions added. The result of study herein is consistent with these spectroscopy measurements. More importantly, it reveals the molecular mechanism underlying, and therefore provides valuable insights into the general hydration dynamics and solvation effect in the concentrated ionic solutions as well as the confined environment with explicit charges presented.

Methods

1. The CTRW Coarse-Graining Method. We apply a coarse-graining time algorithm (17) to the single-molecule water trajectories to quantitatively rationalize the magnitude and concentration dependences of the hopping time τ_{RW} and jump length, L_{RW}. In this algorithm, the center of the *k*th dynamic basin of the tagged water molecule, $\bar{R}(n)_k$, is the running average of the molecular center-of-mass $\bar{R}(n)$:

$$\bar{R}(n)_k = \frac{(n-1)\bar{R}(n-1)_k + R(n)}{n}. \quad [5]$$

The average is updated until $R(n+1)$ walks out of a certain range:

$$\left|R(n+1) - \bar{R}(n)_k\right| \begin{cases} \le D_{\max} & \text{update the basin center position} \\ > D_{\max} & \text{start the new basin} \end{cases}. \quad [6]$$

We set $D_{\max} = 1.5$ Å (17), which was found to be a reasonable value for the pure water, as a threshold of the basin crossing. The past *n* snapshots are defined as a dynamical basin centered at $\bar{R}(n)_k$. If the labeled molecule hops into a new basin according to Eq. **6**, the running index *n* is updated to 1. The hopping time τ_{RW} is defined as the average waiting time of water within

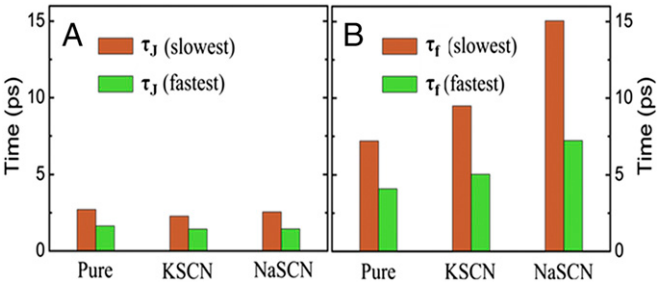

Fig. 7. The jump (*A*) and frame (*B*) rotational times (*B*) of the slowest and the fastest water in KSCN and NaSCN solutions at 5 M. Target water molecules are selected according to the population function of Eq. **2**. Their jump rotational times are calculated by Eqs. **S4a** and **S4b**, and their frame rotational times are obtained by fitting the $C_f(t)$ in Eq. **S2** with single-exponential function.

dynamic basin $\bar{R}(n)_k$, while the jump length L_{RW} is the average distance between two consecutive basin centers, $\langle \bar{R}_{k+1} - \bar{R}_K \rangle$.

2. Van Hove Distribution Function. We introduce the self-part rotational van Hove distribution function (24),

$$G_R(\phi, t) = \left\langle \frac{1}{N} \sum_{i=1}^{N} \delta\left(\left| \bar{\phi}_i(t) - \bar{\phi}_i(0) \right| - \phi \right) \right\rangle, \quad [7]$$

where $\langle \cdots \rangle$ represents average over configurations. With this formalism, we recover the usual interpretation for $4\pi\phi^2 G_R(\phi, t)$ as the probability of having a molecule at time t with angular displacement. For long times, the diffusion equation for $\bar{\phi}(t)$ holds, and $G_R(\phi, t)$ are Gaussian distribution $G_0(\phi, t)$:

$$G_0(\phi, t) = \left[\frac{3}{2\pi \langle \phi^2(t) \rangle} \right]^{3/2} \exp\left[-3\phi^2 / 2\langle \phi^2(t) \rangle \right]. \quad [8]$$

The deviation of $G_R(\phi, t)$ from $G_0(\phi, t)$ can be quantified by the non-Gaussian parameter. The $\alpha_2(t)$ in pure water, KSCN solution, and NaSCN solution at 5 M are presented in Fig. 5:

$$\alpha_2(t) = 3\langle \phi^4(t) \rangle / 5\langle \phi^2(t) \rangle^2 - 1.$$

3. Ion Cluster and Hydrogen Bond Definitions. We define the ion cluster as follows (18): (*i*) every ion X is connected to at least one counterion Y of the opposite charge; two ions are said to be connected if they are separated by a distance $R_{X\text{-}Y}$ smaller than the separation d corresponding to the first minimum of the pair radial distribution function; (*ii*) every ion can be reached from any other ion within the cluster through a path of consecutive connections. The total number of all of the ions in each ion cluster is defined as the size of ion cluster.

Two water molecules are considered to be hydrogen bonded if the distance between their oxygens $R_{OwOw} < 3.5$ Å, and the angle $\theta_{HOwOw} < 30°$ (O_w: water oxygen atom; H_w: water hydrogen atom).

4. The Populations of the Rotational Angle of Ion Cluster. The rotational angle of ion cluster is calculated by the superposition method (31). We take two structures of ion cluster at time $t = t_0$ and $t = t_1$ along a continuous MD trajectory. The mass centers of ion clusters at two times are overlapped by a translational transformation, and then superimpose them by a rotation operation with a rotational angle in the optimal least-squares sense, if the ion cluster is intact during the interval $\Delta t = t_1 - t_0$. Due to the dissociation and association during the interval, if the 80% of ion in the ion cluster at $t = t_0$ is remained continuously at $t = t_1$, the ion cluster is thought as an intact ion cluster. The ion cluster is classified into two classes. One is small ion cluster with the size $2 < N < 10$. The other is the big ion cluster with the size not less than 10.

Supporting Information. *Supporting Information* includes details of the experiments and simulation, the rotational correlation functions, the extended Ivanov jump model, the CTRW coarse-graining method, van Hove distribution function, the rotation of ion cluster, table, and figures.

ACKNOWLEDGMENTS. This material is based upon work supported by the National Key Research and Development Program of China (2017YFA0206801), the Strategic Priority Research Program of the Chinese Academy of Sciences (XDB20000000 and XDB10040304), and National Natural Science Foundation of China Grants 21373201 and 21433014. Q.Z. is grateful for the support of Scientific Research Foundation for Returned Scholars, Ministry of Education of China, and Liaoning BaiQianWan Talents Program (2015-294). S.M. acknowledges the support of NSF Grant CHE-1361516.

1. Bakker HJ (2008) Structural dynamics of aqueous salt solutions. *Chem Rev* 108: 1456–1473.
2. Laage D, Elsaesser T, Hynes JT (2017) Water dynamics in the hydration shells of biomolecules. *Chem Rev* 117:10694–10725.
3. Bellissent-Funel MC, et al. (2016) Water determines the structure and dynamics of proteins. *Chem Rev* 116:7673–7697.
4. Qin Y, Wang L, Zhong D (2016) Dynamics and mechanism of ultrafast water–protein interactions. *Proc Natl Acad Sci USA* 113:8424–8429.
5. Levy Y, Onuchic JN (2006) Water mediation in protein folding and molecular recognition. *Annu Rev Biophys Biomol Struct* 35:389–415.
6. Zhang Q, et al. (2017) The opposite effects of sodium and potassium cations on water dynamics. *Chem Sci* 8:1429–1435.
7. Gertner BJ, Whitnell RM, Wilson KR, Hynes JT (1991) Activation to the transition state: Reactant and solvent energy flow for a model SN2 reaction in water. *J Am Chem Soc* 113:74–87.
8. Miller JR, Simon P (2008) Materials science. Electrochemical capacitors for energy management. *Science* 321:651–652.
9. Smith L, Dunn B (2015) Batteries. Opening the window for aqueous electrolytes. *Science* 350:918.
10. Guo GC, Yao YG, Wu KC, Wu L, Huang JS (2001) Fundamental research on the structure sensitive functional materials. *Huaxue Jinzhan* 13:151–155.
11. Stirnemann G, Wernersson E, Jungwirth P, Laage D (2013) Mechanisms of acceleration and retardation of water dynamics by ions. *J Am Chem Soc* 135:11824–11831.
12. Bian HT, et al. (2011) Ion clustering in aqueous solutions probed with vibrational energy transfer. *Proc Natl Acad Sci USA* 108:4737–4742.
13. Tielrooij KJ, Garcia-Araez N, Bonn M, Bakker HJ (2010) Cooperativity in ion hydration. *Science* 328:1006–1009.
14. Marcus Y, Hefter G (2006) Ion pairing. *Chem Rev* 106:4585–4621.
15. Laage D, Hynes JT (2006) A molecular jump mechanism of water reorientation. *Science* 311:832–835.
16. Leberman R, Soper AK (1995) Effect of high salt concentrations on water structure. *Nature* 378:364–366.
17. Qvist J, Schober H, Halle B (2011) Structural dynamics of supercooled water from quasielastic neutron scattering and molecular simulations. *J Chem Phys* 134:144508.
18. Zhang Q, et al. (2013) Microscopic origin of the deviation from Stokes-Einstein behavior observed in dynamics of the KSCN aqueous solutions: A MD simulation study. *J Phys Chem B* 117:2992–3004.
19. Ohmine I, Saito S (1999) Water dynamics: Fluctuation, relaxation, and chemical reactions in hydrogen bond network rearrangement. *Acc Chem Res* 32:825–825.
20. Georgalis Y, Kierzek AM, Saenger W (2000) Cluster formation in aqueous electrolyte solutions observed by dynamic light scattering. *J Phys Chem B* 104:3405–3406.
21. Kim S, Kim H, Choi JH, Cho M (2014) Ion aggregation in high salt solutions: Ion network versus ion cluster. *J Chem Phys* 141:124510.
22. Shen Y, et al. (2015) Comparison studies on sub-nanometer-sized ion clusters in aqueous solutions: Vibrational energy transfers, MD simulations, and neutron scattering. *J Phys Chem B* 119:9893–9904.
23. Bian H, et al. (2013) Cation effects on rotational dynamics of anions and water molecules in alkali (Li^+, Na^+, K^+, Cs^+) thiocyanate (SCN^-) aqueous solutions. *J Phys Chem B* 117:7972–7984.
24. Marcus Y (2009) Effect of ions on the structure of water: Structure making and breaking. *Chem Rev* 109:1346–1370.
25. Kincaid JF, Eyring H, Stearn AE (1941) The theory of absolute reaction rates and its application to viscosity and diffusion in the liquid state. *Chem Rev* 28:301–365.
26. Mazza MG, Giovambattista N, Starr FW, Stanley HE (2006) Relation between rotational and translational dynamic heterogeneities in water. *Phys Rev Lett* 96:057803.
27. Laage D, Hynes JT (2007) Reorientional dynamics of water molecules in anionic hydration shells. *Proc Natl Acad Sci USA* 104:11167–11172.
28. Li P, Merz KM, Jr (2017) Metal ion modeling using classical mechanics. *Chem Rev* 117: 1564–1686.
29. VandeVondele J, et al. (2005) QUICKSTEP: Fast and accurate density functional calculations using a mixed Gaussian and plane waves approach. *Comput Phys Commun* 167:103–128.
30. Jungwirth P (2015) Biological water or rather water in biology? *J Phys Chem Lett* 6: 2449–2451.
31. Kearsley SK (1989) On the orthogonal transformation used for structural comparisons. *Acta Crystallogr A* 45:208–210.
32. Wallace AF, et al. (2013) Microscopic evidence for liquid–liquid separation in supersaturated $CaCO_3$ solutions. *Science* 341:885–889.
33. Zhang R, Zhuang W (2013) Effect of ion pairing on the solution dynamics investigated by the simulations of the optical Kerr effect and the dielectric relaxation spectra. *J Phys Chem B* 117:15395–15406.
34. Lee SH, Rasaiah JC (1996) Molecular dynamics simulation of ion mobility. 2. Alkali metal and halide ions using the SPC-E model for water at 25 °C. *J Phys Chem* 100: 1420–1425.
35. Vincze Á, Jedlovszky P, Horvai G (2002) The L/L interface and adsorption of SCN- anions as studied by different molecular simulation techniques. *Analytical Sciences/ Supplements Proceedings of IUPAC International Congress on Analytical Sciences 2001 (ICAS 2001)* (The Japan Society for Analytical Chemistry, Tokyo), i317–i320.
36. Mason PE, et al. (2004) The structure of aqueous guanidinium chloride solutions. *J Am Chem Soc* 126:11462–11470.
37. Aqvist J (1990) Ion-water interaction potentials derived from free energy perturbation simulations. *J Phys Chem* 94:8021–8024.
38. Berendsen HJC, Grigera JR, Straatsma TPJ (1987) The missing term in effective pair potentials. *J Phys Chem* 91:6269–6271.
39. Ponder JW, Richards FM (1987) An efficient Newton-like method for molecular mechanics energy minimization of large molecules. *J Comput Chem* 8:1016–1026.
40. Van Der Spoel D, et al. (2005) GROMACS: Fast, flexible, and free. *J Comput Chem* 26: 1701–1718.